

## **Supplementary Information**

# **Unique Proton Transportation Pathway in a Robust Inorganic Coordination Polymer Leading to Intrinsically High and Sustainable Anhydrous Proton Conductivity**

**Daxiang Gui,<sup>1#</sup> Xing Dai,<sup>1#</sup> Zetian Tao,<sup>2#</sup> Tao Zheng,<sup>1</sup> Xiangxiang Wang,<sup>1</sup> Mark A. Silver,<sup>1</sup> Jie Shu,<sup>3</sup> Lanhua Chen,<sup>1</sup> Yanlong Wang,<sup>1</sup> Tiantian Zhang,<sup>3</sup> Jian Xie,<sup>1</sup> Lin Zou,<sup>4</sup> Yuanhua Xia,<sup>4</sup> Jujia Zhang,<sup>5</sup> Jin Zhang,<sup>5</sup> Ling Zhao,<sup>6\*</sup> Juan Diwu,<sup>1</sup> Ruhong Zhou,<sup>1,7\*</sup> Zhifang Chai,<sup>1</sup> and Shuaow Wang<sup>1\*</sup>**

<sup>1</sup>State Key Laboratory of Radiation Medicine and Protection, School for Radiological and interdisciplinary Sciences (RAD-X) and Collaborative Innovation Centre of Radiation Medicine of Jiangsu Higher Education Institutions, Soochow University, Suzhou 215123, China

<sup>2</sup>Key Laboratory for Advanced Technology in Environmental Protection of Jiangsu Province, Yancheng Institute of Technology, Yancheng 224001, Jiangsu China

<sup>3</sup>Analysis and Testing Center, Soochow University, 199 Renai Road, Suzhou 215123, China

<sup>4</sup>Key Laboratory of Neutron Physics and Institute of Nuclear Physics and Chemistry, China Academy of Engineering Physics(CAEP), Mianyang 621999, China

<sup>5</sup>Beijing Key Lab of Bio-inspired Energy Materials and Devices & School of Space and Environment, Beihang University, Beijing 100191, China.

<sup>6</sup>Department of Material Science and Chemistry, China University of Geosciences, Wuhan 430074, China.

<sup>7</sup>Computational Biology Center, IBM Thomas J Watson Research Center, Yorktown Heights, NY 10598; Department of Chemistry, Columbia University, New York, NY 10027, United States.

## Supplementary Figures

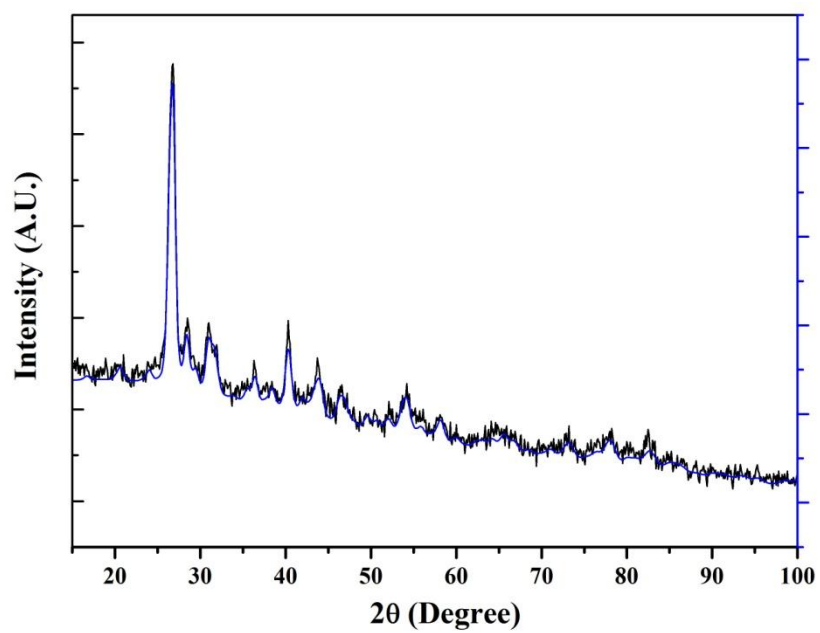


**Figure S1.** Neutron powder diffraction patterns of **ZrP** after refinement at room temperature.

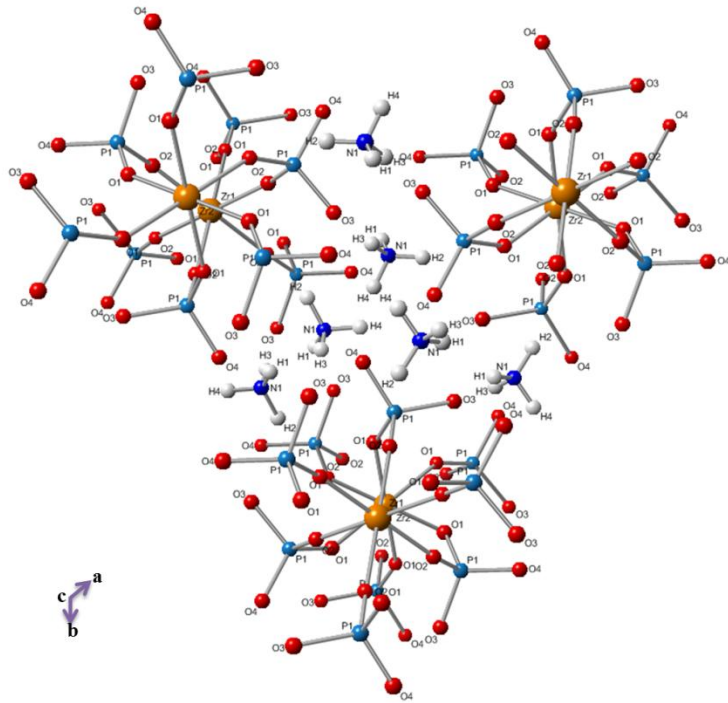
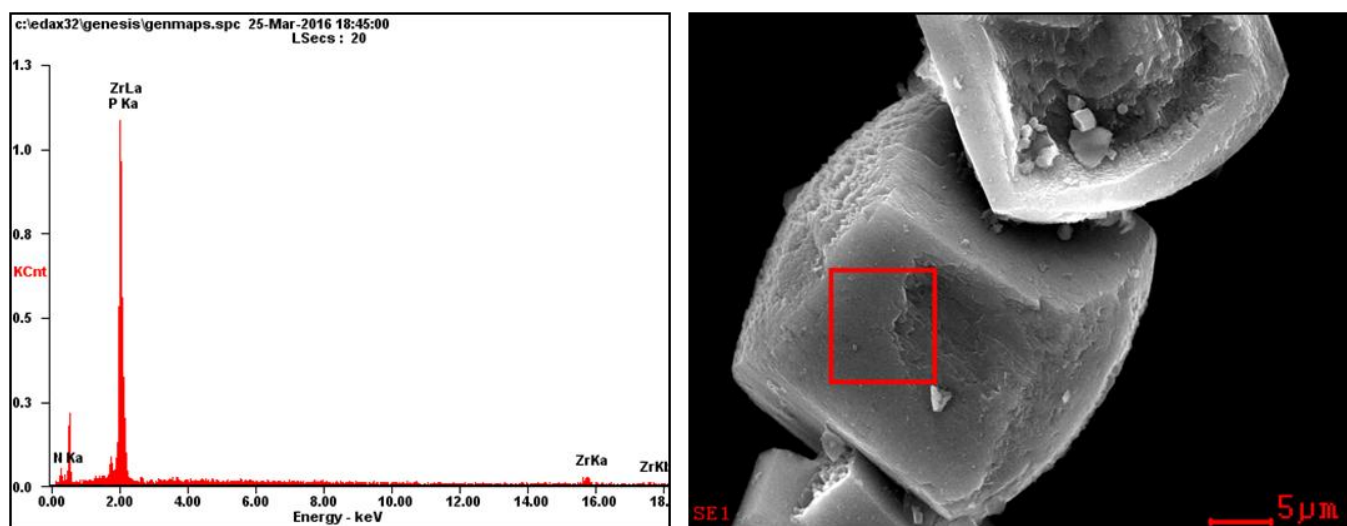


**Figure S2.** Neutron powder diffraction simulation structure of **ZrP** after refinement at room temperature.



<i>Element</i>	<i>Wt%</i>	<i>At%</i>
<i>NK</i>	10.63	18.29
<i>OK</i>	38.00	57.23
<i>PK</i>	21.24	16.52
<i>ZrK</i>	30.13	07.96
<i>Matrix</i>	Correction	ZAF

**Figure S3.** EDS (a) and SEM (b) analysis of **ZrP**.

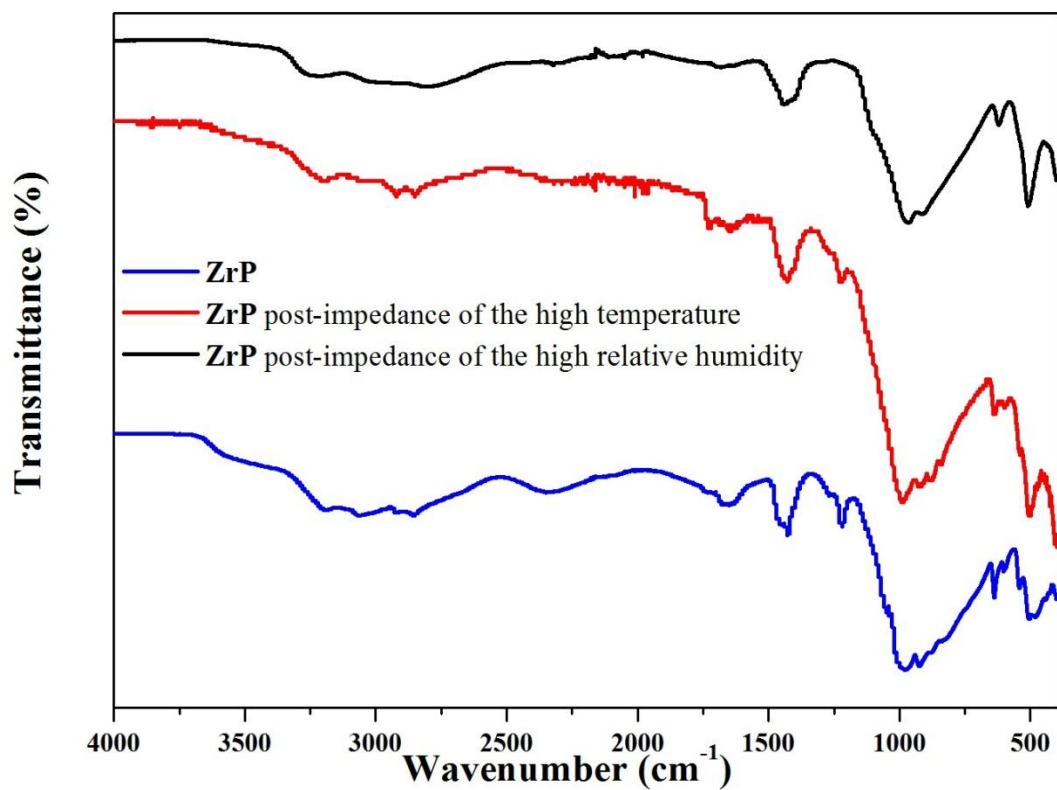


**Figure S4.** FT-IR spectra of **ZrP** (black) and **ZrP** after the time-dependent conductivity measurement (red and blue)

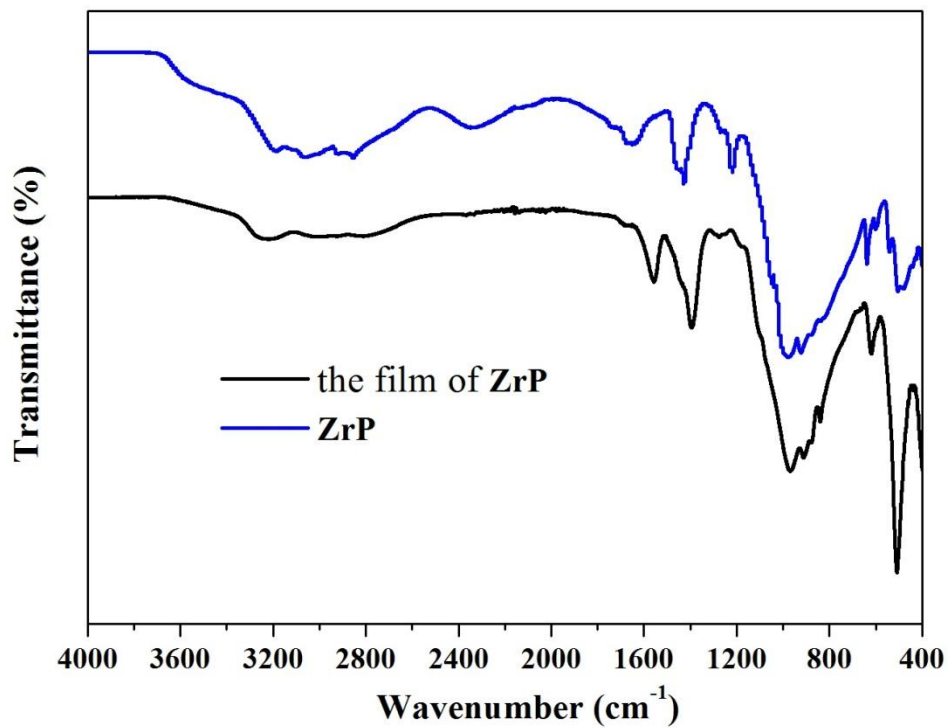


**Figure S5.** FT-IR spectra of **ZrP** (blue) and the film of **ZrP** (black) used for the fuel cell assembly.

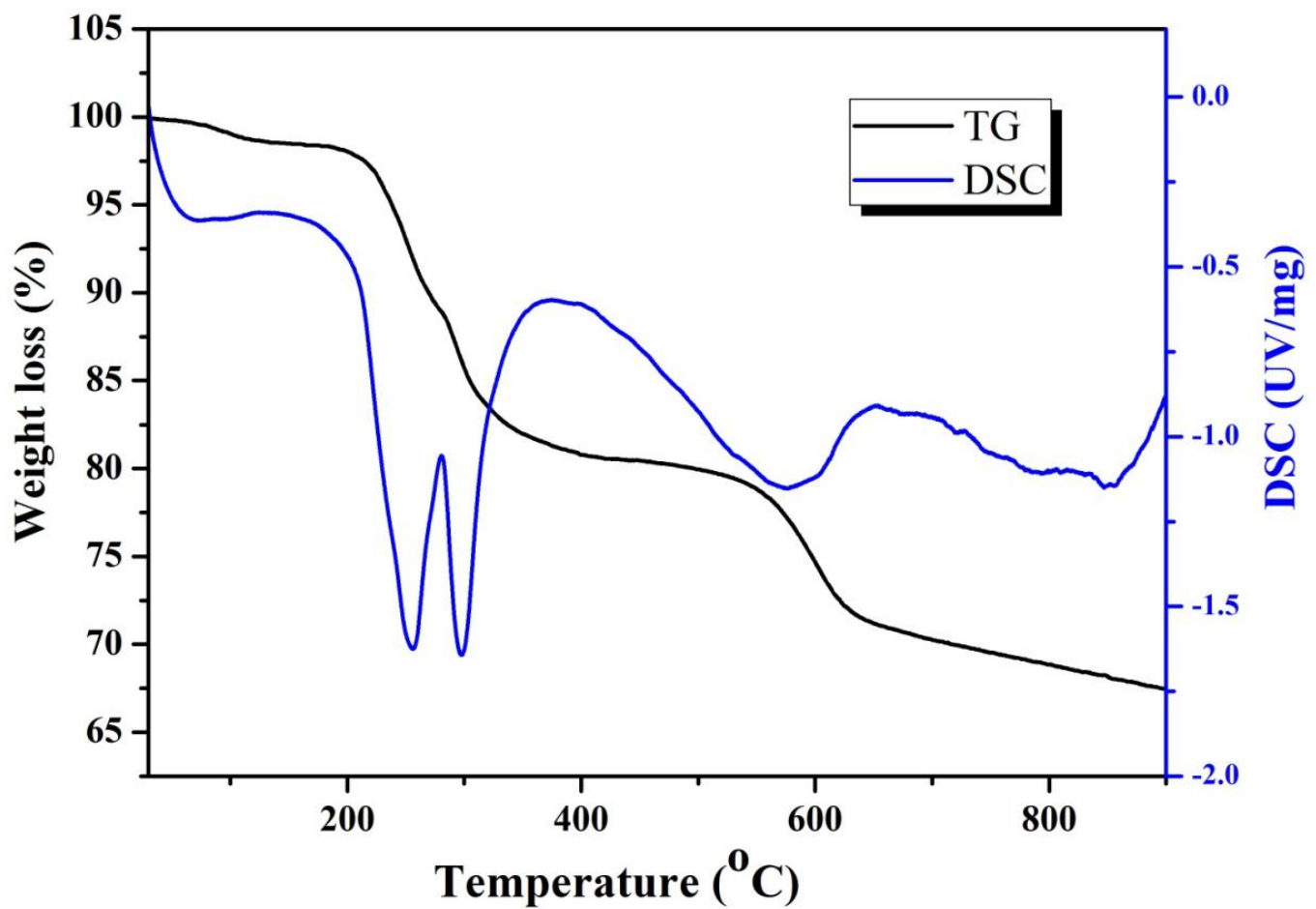


**Figure S6.** TGA and DSC curve of ZrP measured from 30 to 900 °C in the nitrogen atmosphere.

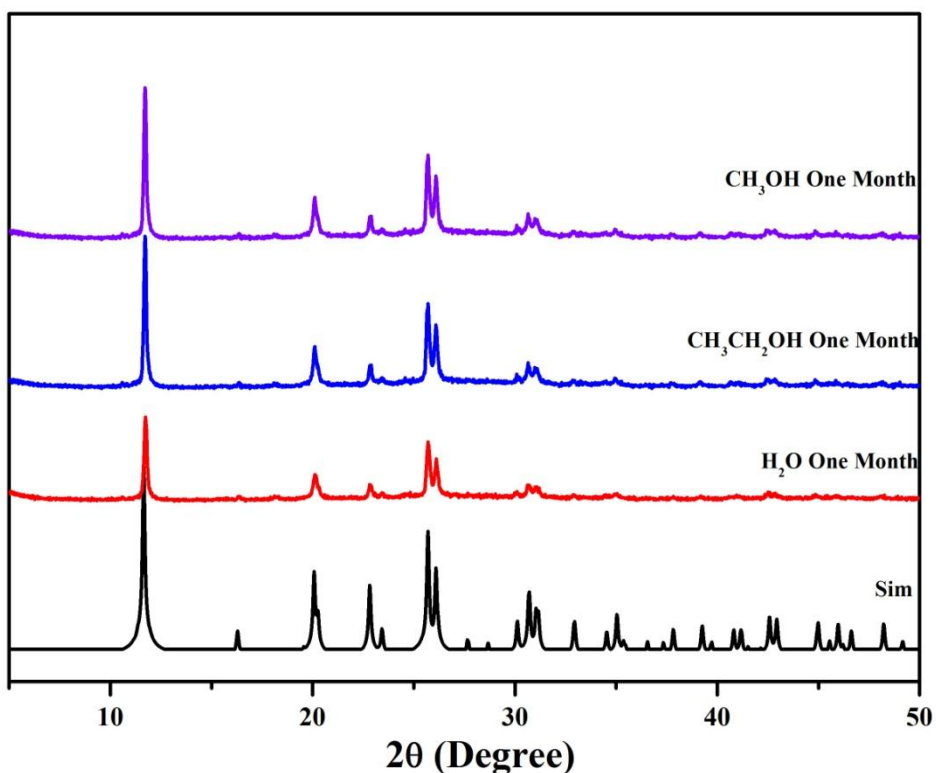


**Figure S7.** Simulated and experimental PXRD patterns of **ZrP** and **ZrP** soaked in a variety of solutions.

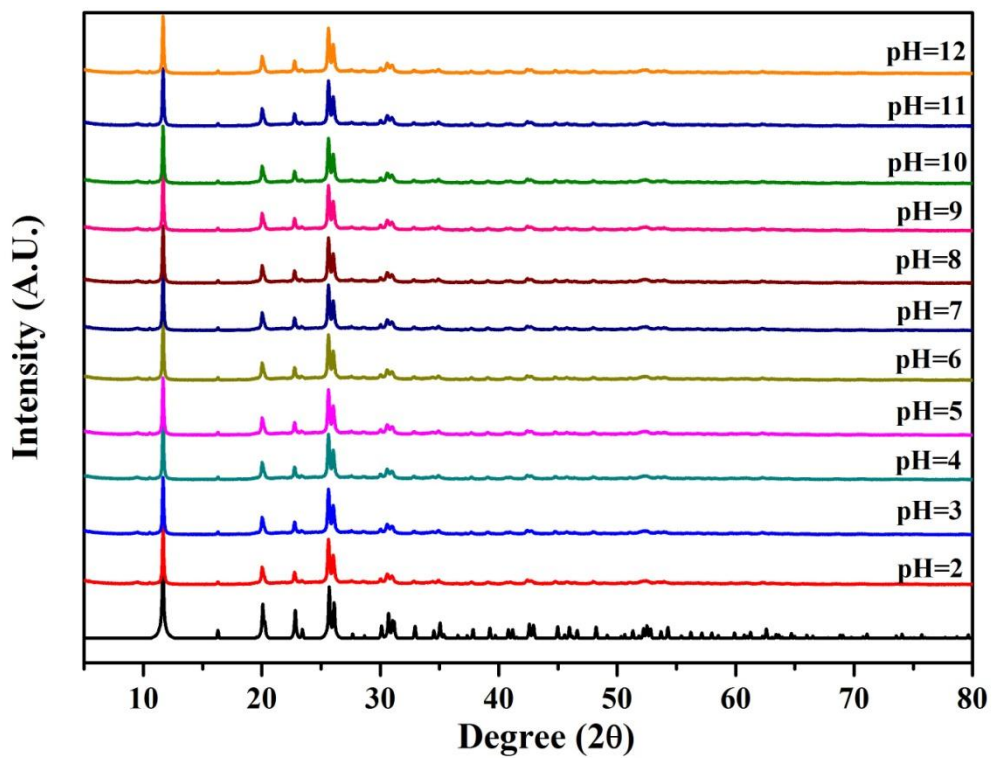


**Figure S8.** Simulated and experimental PXRD patterns for **ZrP** and for **ZrP** soaked in aqueous solutions at pH 2-12 for 72 h.

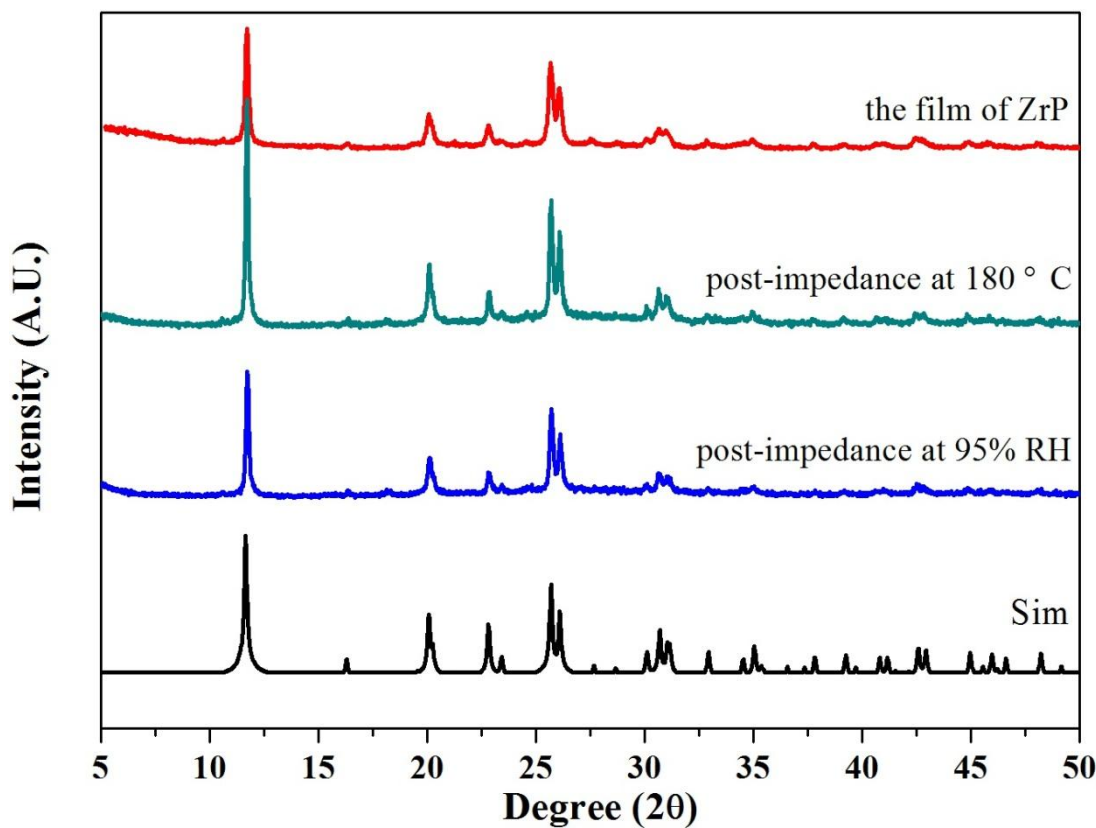


**Figure S9.** Simulated and experimental PXRD patterns of **ZrP**, **ZrP** for post-impedance measurement, and the film of **ZrP** (black) used for the fuel cell assembly.

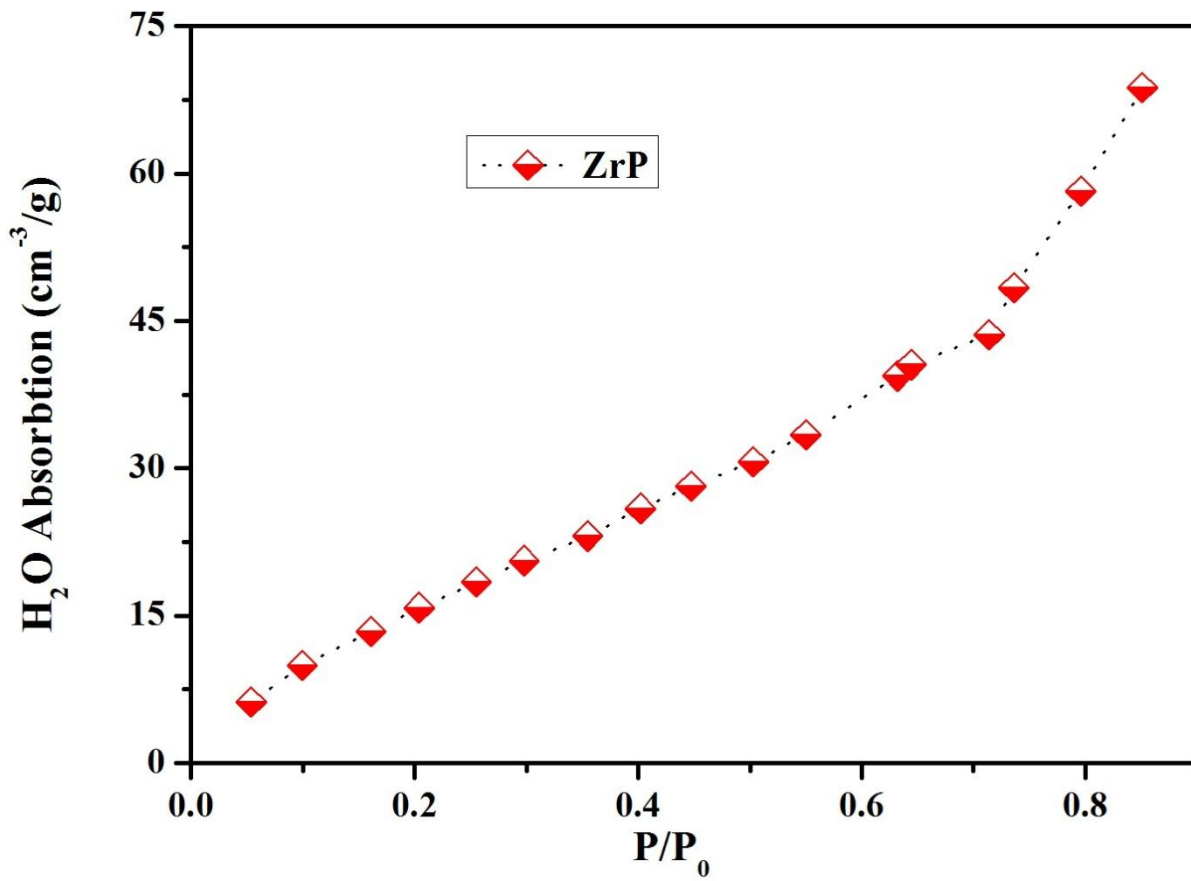


**Figure S10.** Water vapor adsorption isotherms of dispersed crystals of **ZrP** measured at 298 K.

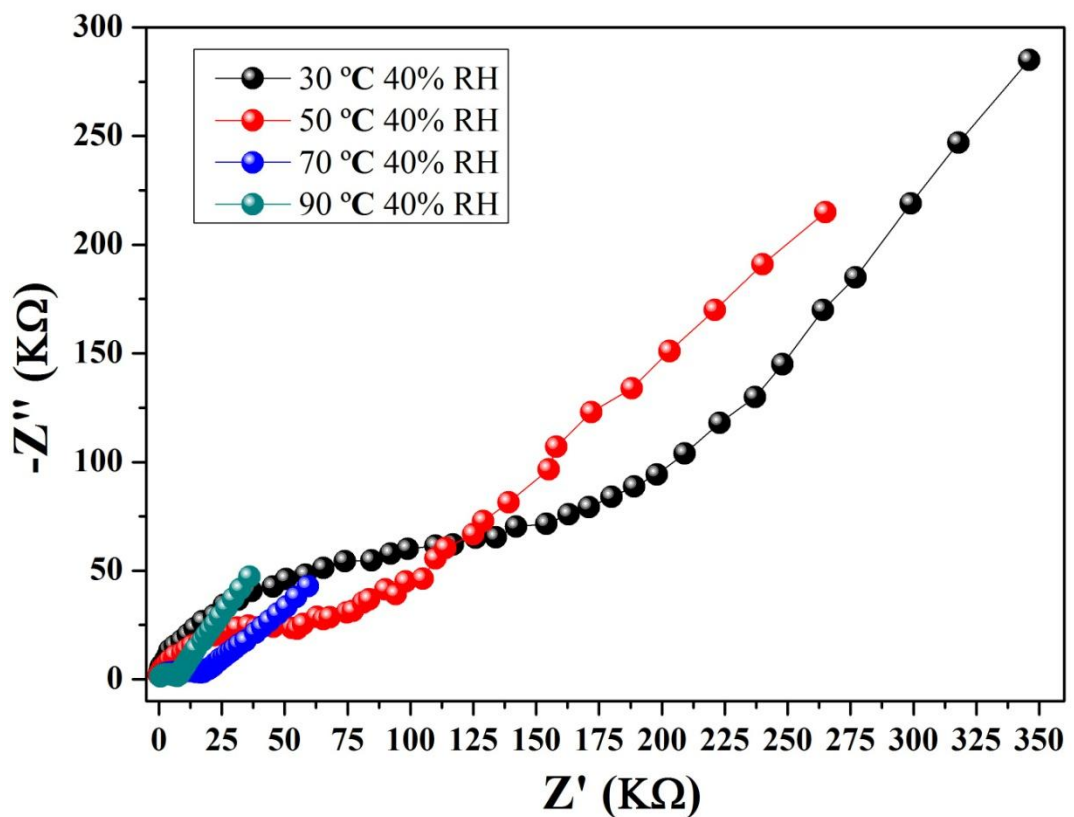


**Figure S11.** Impedance plots of **ZrP** at different temperatures under 40% RH.

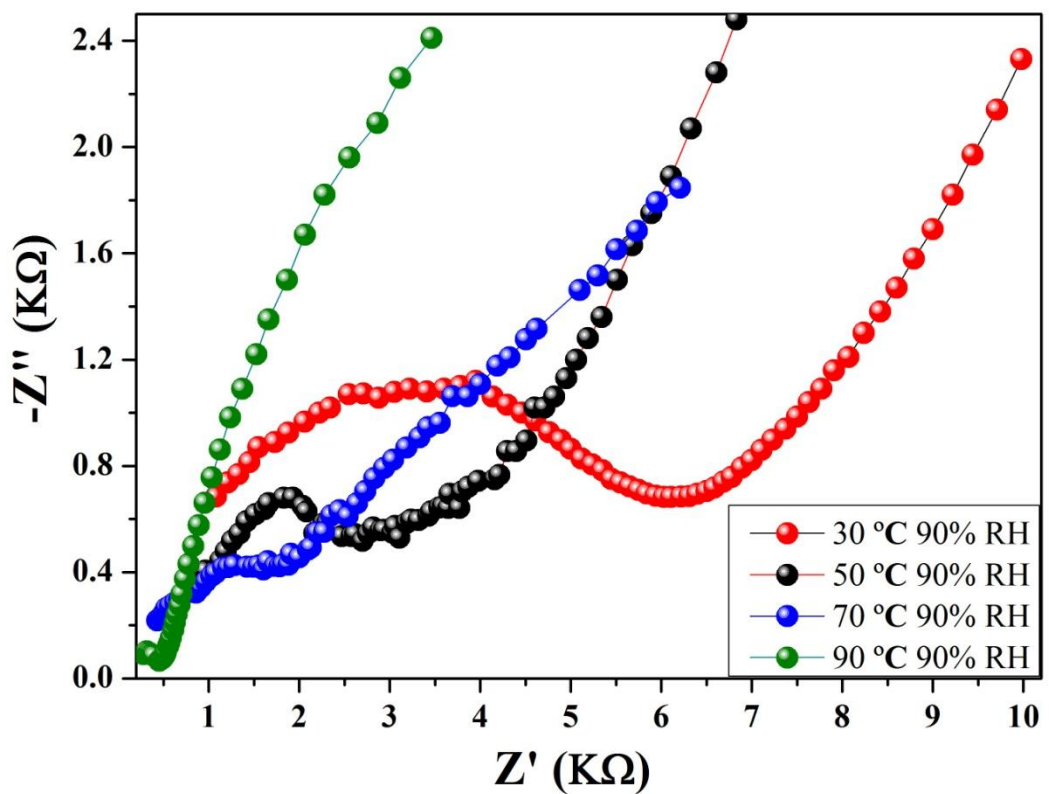


**Figure S12.** Impedance plots of **ZrP** at different temperatures under 90% RH.

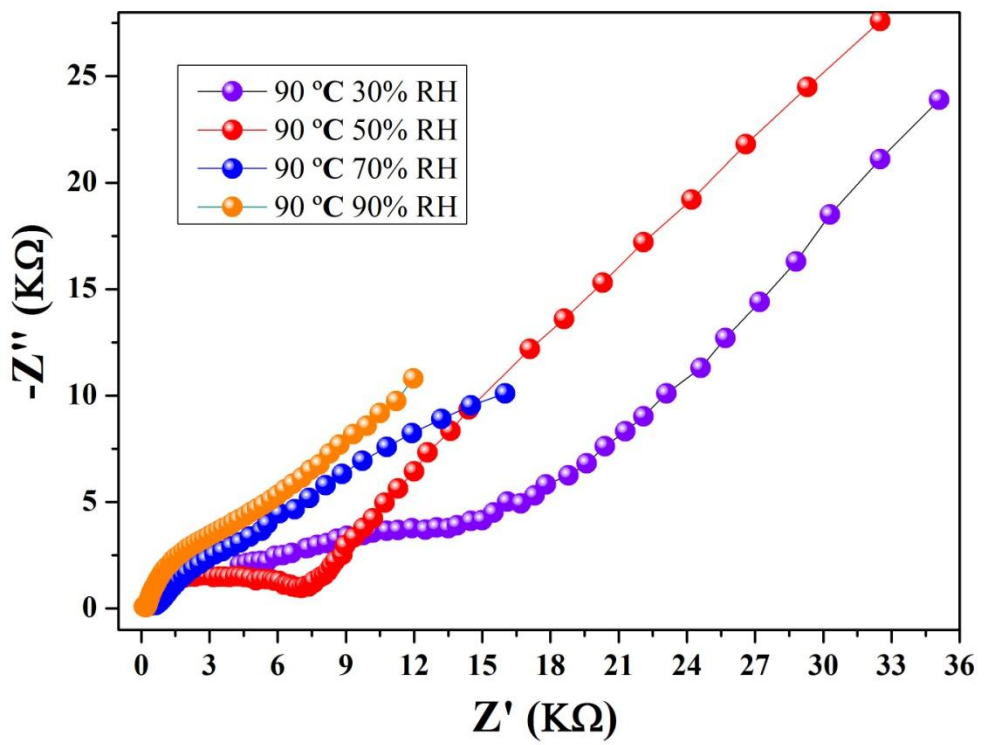


**Figure S13.** Impedance plots of **ZrP** at different relative humidity under 90 °C.

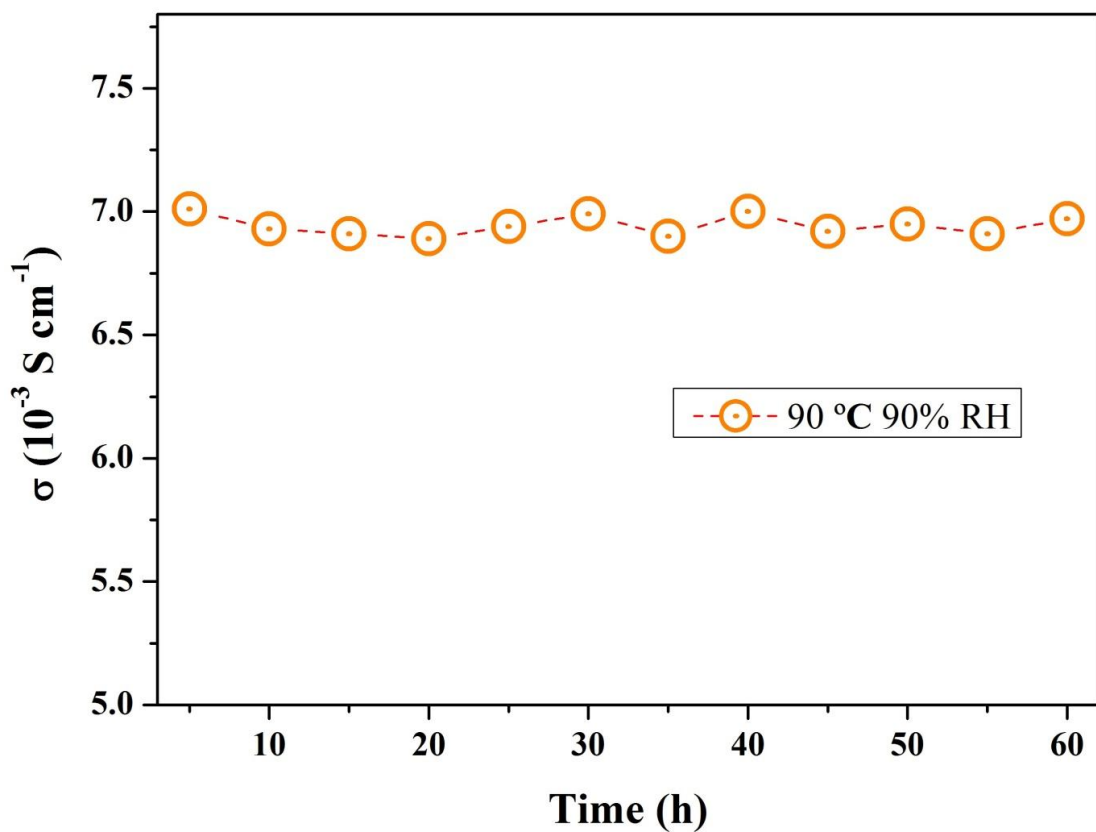


**Figure S14.** Time-dependent proton conductivities of **ZrP** at 90 °C and 90% RH.

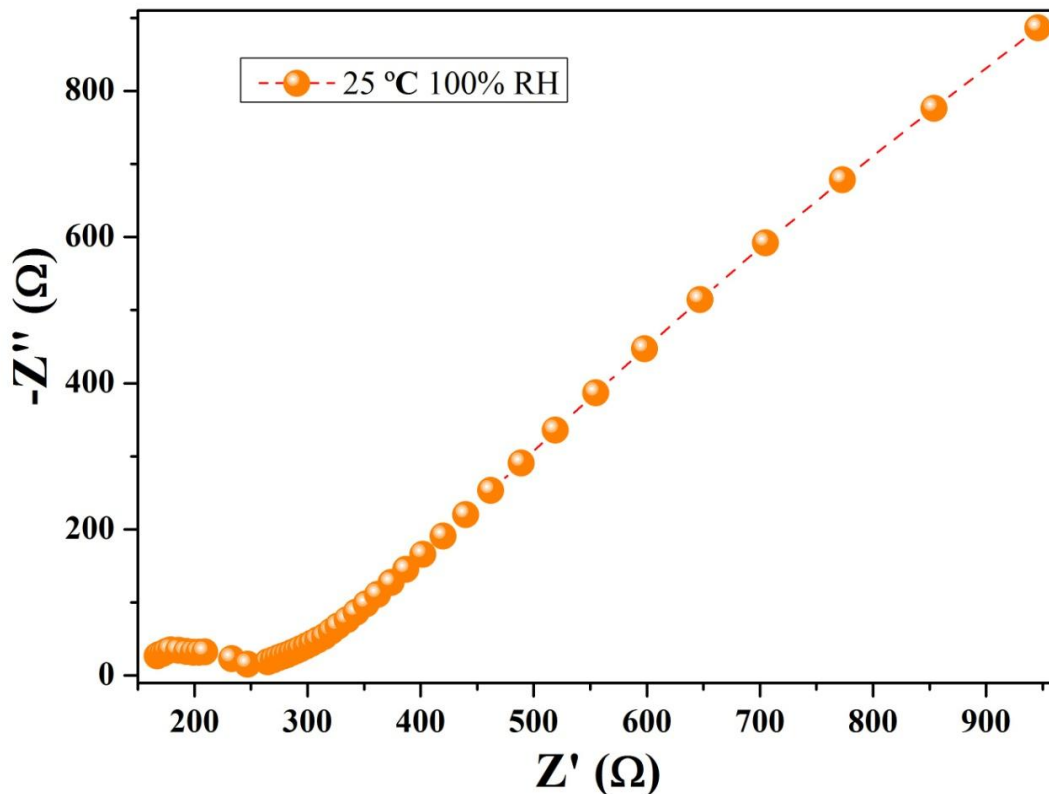


**Figure S15.** Impedance plots of **ZrP** at 25 °C and 100% RH.

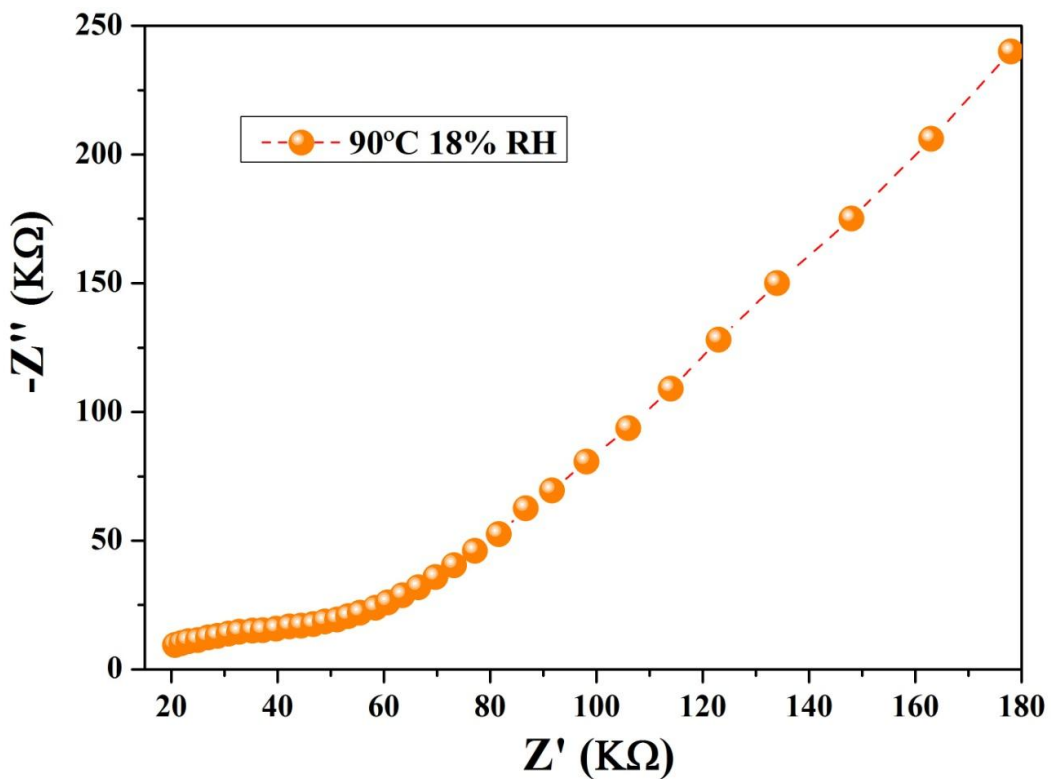


**Figure S16.** Impedance plots of **ZrP** at 90 °C and 18% RH.

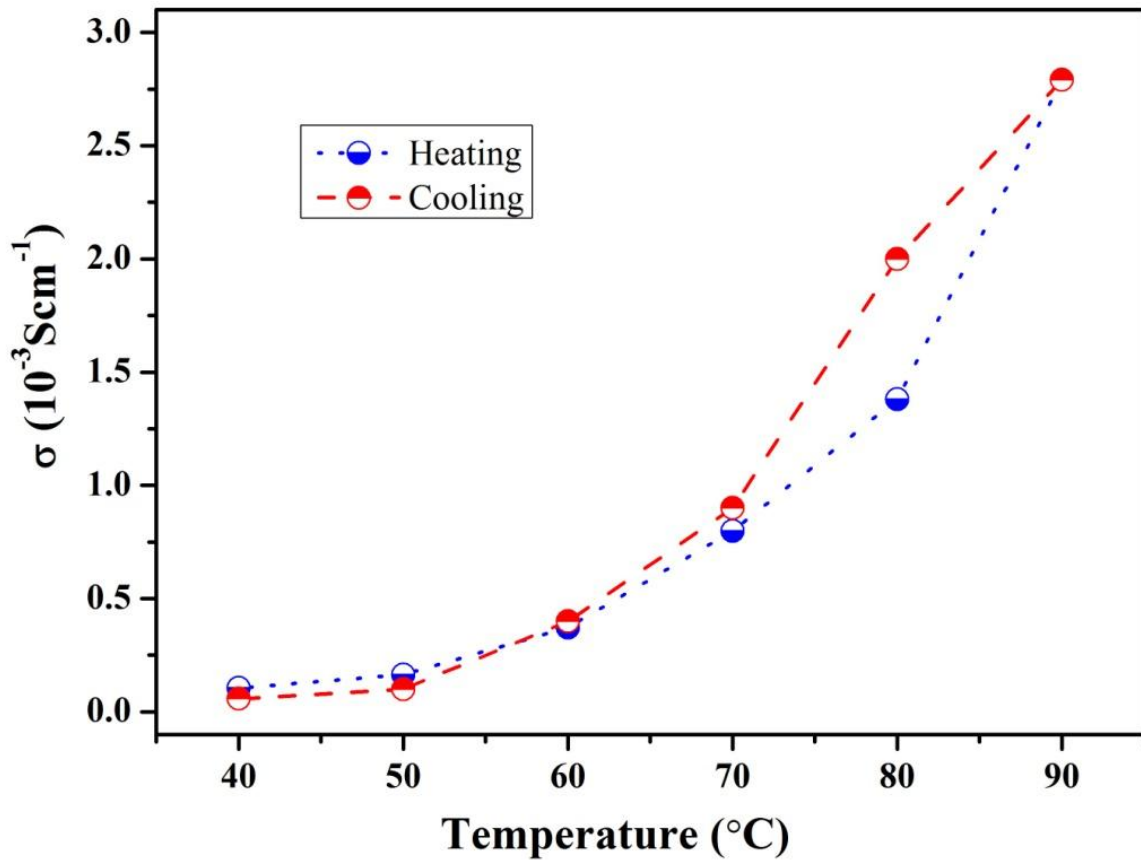


**Figure S17.** Heating (blue line) and cooling (red line) cycles of **ZrP** showing almost overlapped dependent conductivity values at different temperatures under 90% RH.

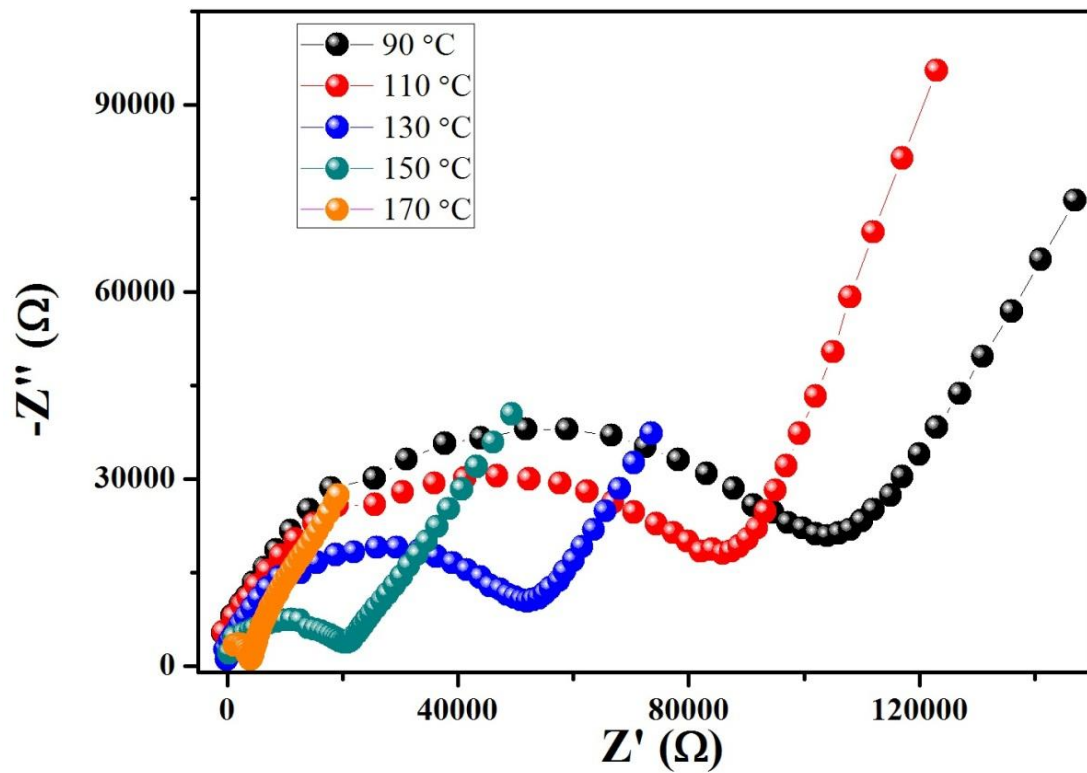


**Figure S18.** Impedance plots of **ZrP** at different temperatures under zero-humidity.

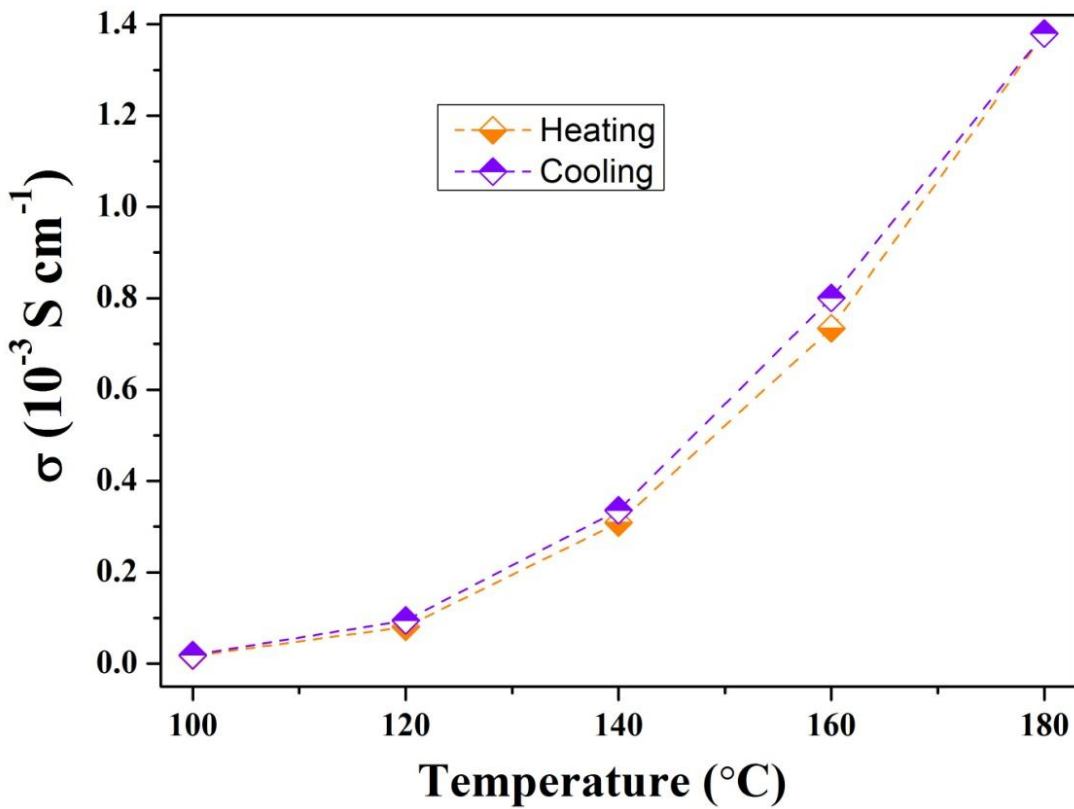


**Figure S19.** Heating (yellow line) and cooling (purple line) cycles of **ZrP** showing almost overlapped dependent conductivity values at different temperatures under zero-humidity.

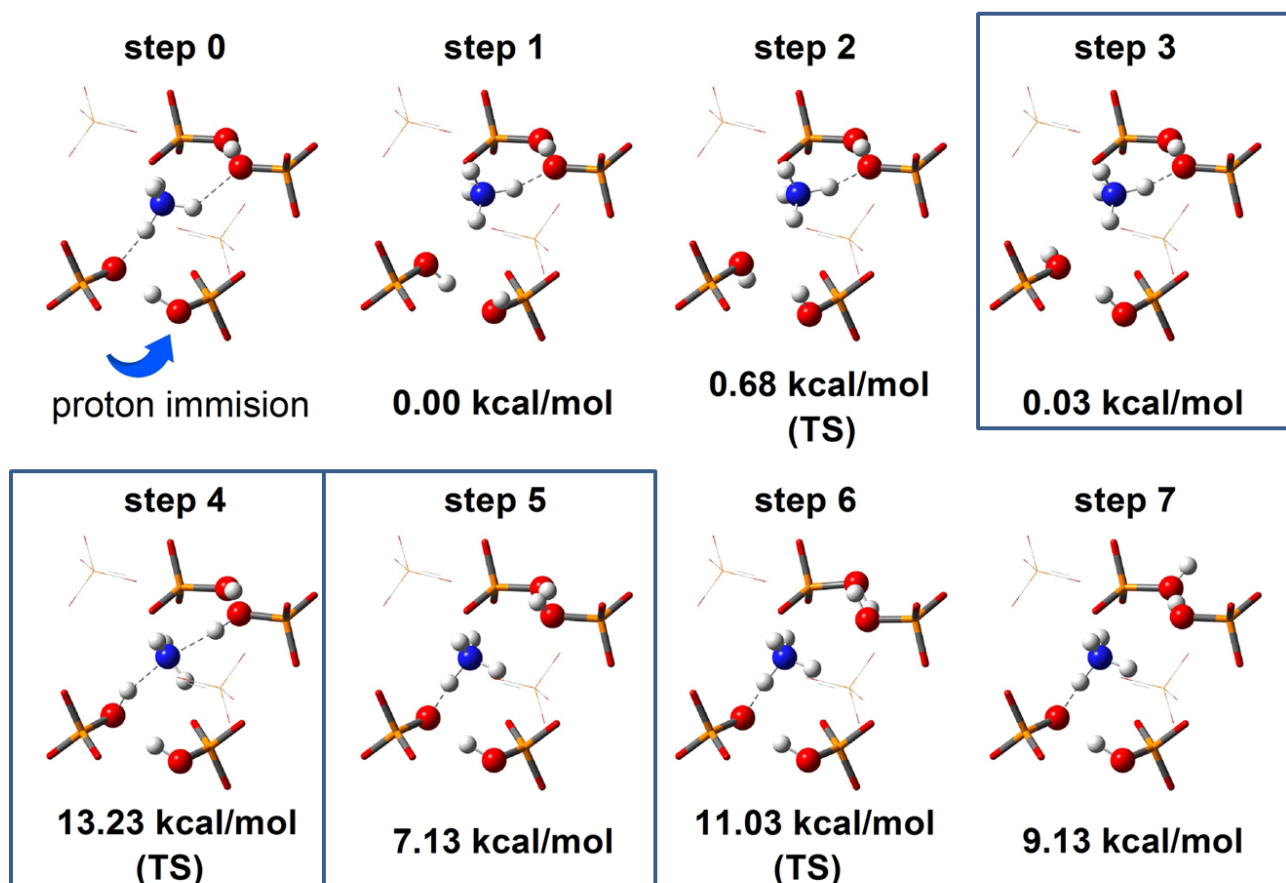


**Figure S20.** DFT calculations on the reaction potential energy surface during proton transfer process.

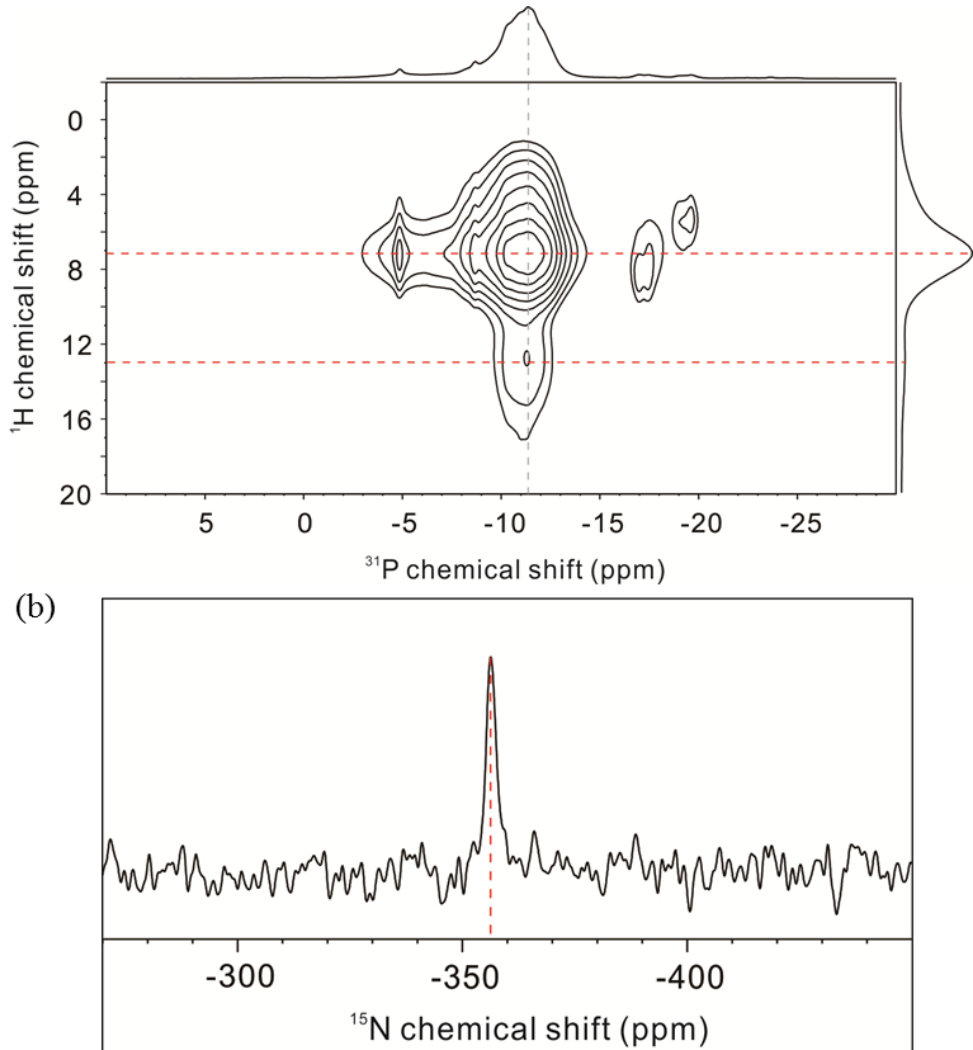


**Figure S21.** (a) 2D  $^1\text{H}$ - $^{31}\text{P}$  exchange SSNMR spectrum, showing the intense cross peaks labeled between  $^{31}\text{P}$  11.42 ppm and  $^1\text{H}$  13.57 ppm, 7.34 ppm. (b) Line shape analysis of the 1D  $^{15}\text{N}$  spectrum, showing one type of  $\text{NH}_4^+$  in the structure.

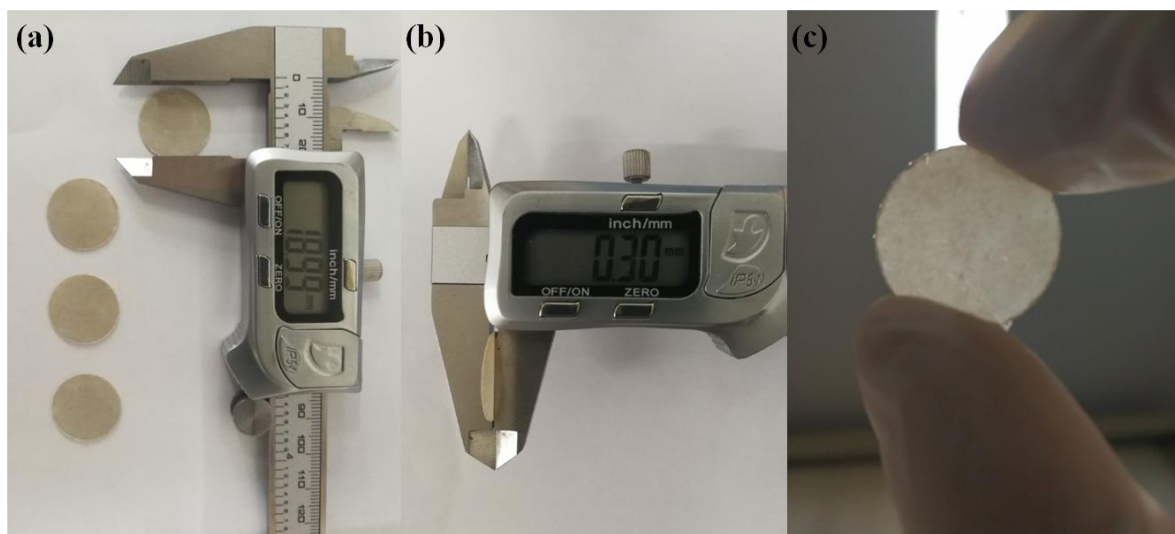


**Figure S22.** The photograph of pressed circular plate of **ZrP** for cell performance and durability test.

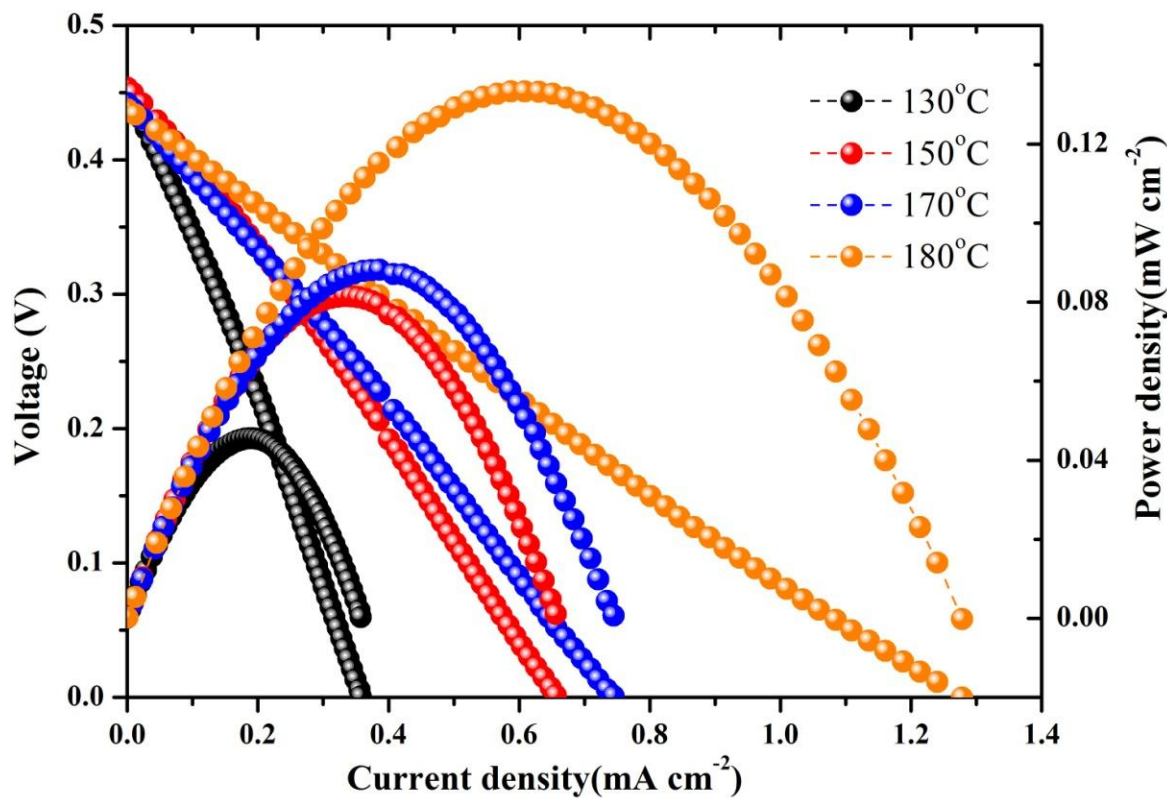


**Figure S23.** Performance of direct methanol fuel cell. Black and blue lines represent current–voltage and current–power, respectively.

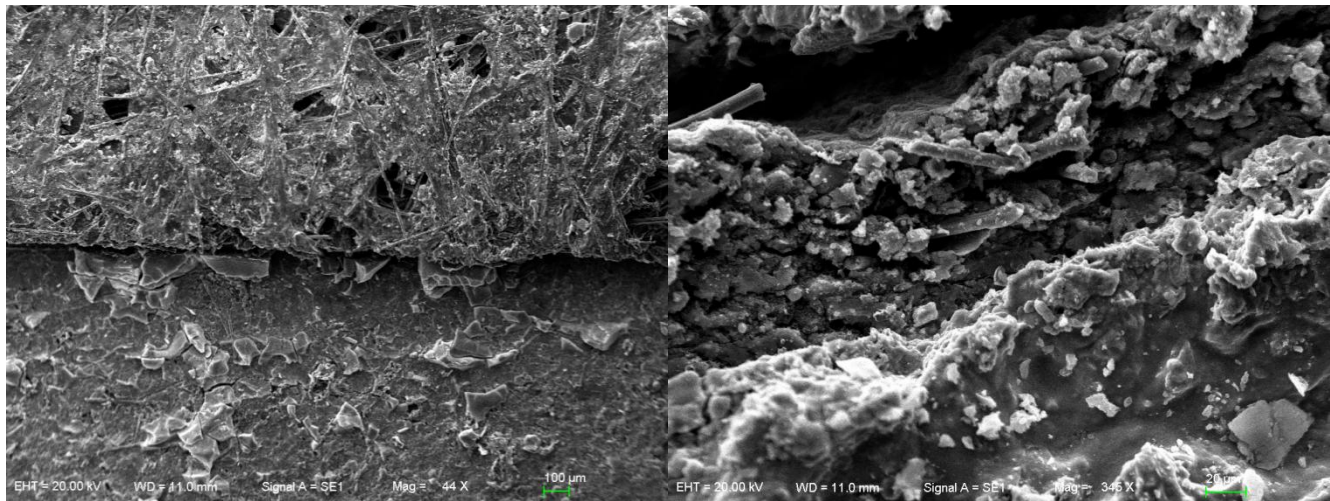


**Figure S24.** The SEM photo of pressed circular plate of ZrP for cell performance and durability test.

## Supplementary Table

**Table S1.** Crystal data and structure refinement results for **ZrP**.

compounds	ZrP	
Empirical formula	$(\text{NH}_4)_3\text{Zr}(\text{H}_{2/3}\text{PO}_4)_3$	
Formula weight	430.26	
Temperature (K)	123(2)	298(2)
Crystal system	trigonal	
Space group	R-3	
a (Å)	15.1767(12)	15.177(2)
b (Å)	15.1767(12)	15.177(2)
c (Å)	9.6641(16)	9.6641(16)
$\alpha$	90.000	90.000
$\beta$	90.000	90.000
$\gamma$	90.000	90.000
V (Å <sup>3</sup> )	1927.7(4)	1927.8(6)
Z	2	2
D <sub>c</sub> (g cm <sup>-3</sup> )	2.224	2.224
$\mu$ (mm <sup>-1</sup> )	1.294	1.294
F (000)	1284.0	1284.0
GOF on F <sup>2</sup>	1.072	1.029
R <sub>1</sub> , <sup>a</sup> wR <sub>2</sub> <sup>b</sup> (I > 2σ(I))	0.0436, 0.1143	0.0443, 0.1215
R <sub>1</sub> , <sup>a</sup> wR <sub>2</sub> <sup>b</sup> (all data)	0.0634, 0.1208	0.0638, 0.1309
CCDC	1813501	
<sup>a</sup> R <sub>1</sub> = $\sum  F_o  -  F_c  /\sum F_o $ . <sup>b</sup> wR <sub>2</sub> = $[\sum_w(F_o^2 - F_c^2)^2 / \sum_w(F_o^2)^2]^{1/2}$ .		

**Table S2.** Selected bond distances ( $\text{\AA}$ ) of **ZrP** and bond-valence sums ( $\Sigma s$ ).

P1-O1	1.529(5)		
P1-O2	1.518(5)		
P1-O3	1.552(6)	$\Sigma s(\text{P1-O3})$	<b>1.14</b>
P1-O4	1.477(5)	$\Sigma s(\text{P1-O4})$	<b>1.41</b>
O3-O3	2.465		

**Table S3.** Hydrogen bonds distances ( $\text{\AA}$ ) and angles ( $^\circ$ ) of **ZrP**.

	N-H distance ( $\text{\AA}$ )	O-H distance ( $\text{\AA}$ )	N-O distance ( $\text{\AA}$ )	Bond angle( $^\circ$ )
N1-H2 .. O3	0.88(2)	2.37(6)	2.983(10)	127(5)
N1-H3 .. O3	0.86(5)	2.01(5)	2.872(10)	176(9)
N1-H1 .. O4	0.86(6)	2.44(9)	2.976(11)	121(7)
N1-H1 .. O4	0.86(6)	2.22(6)	2.842(10)	129(8)
N1-H4 .. O4	0.86(5)	2.02(5)	2.836(12)	158(8)

**Table S4.** Comparison of proton conductivities in representative CPs/MOFs under anhydrous conditions (including H<sub>2</sub>/O<sub>2</sub> fuel cell power density).

Materials	H <sub>2</sub> /O <sub>2</sub> fuel cell power density (mW cm <sup>-2</sup> )	Proton conductivity (10 <sup>-3</sup> S cm <sup>-1</sup> )	Conditions (°C)	Ref.
ZrP	12	1.45	180	This work
[Zn(H <sub>2</sub> PO <sub>4</sub> ) <sub>2</sub> (C <sub>2</sub> N <sub>3</sub> H <sub>3</sub> ) <sub>2</sub> ]n	2.8	4.6	120	1
HCl $\subset$ (C <sub>2</sub> N <sub>2</sub> H <sub>10</sub> )(C <sub>2</sub> N <sub>2</sub> H <sub>9</sub> ) <sub>2</sub> Cu <sub>8</sub> Sn <sub>3</sub> S <sub>12</sub>	/	30.62	165	2
H <sub>2</sub> SO <sub>4</sub> @MIL-101	/	10	150	3
(EMIm) <sub>2</sub> [Zn(SO <sub>4</sub> ) <sub>2</sub> ]	/	3.80	210	4
[Eu <sub>2</sub> (CO <sub>3</sub> )(ox) <sub>2</sub> (H <sub>2</sub> O) <sub>2</sub> ]·4H <sub>2</sub> O	/	2.08	150	5
[Al(OH)(ndc)] <sub>n</sub> $\subset$ His	/	1.70	150	6
[Zn <sub>3</sub> (H <sub>2</sub> PO <sub>4</sub> ) <sub>6</sub> (H <sub>2</sub> O) <sub>3</sub> ]·Hbim	/	1.30	130	7
(Me <sub>2</sub> NH <sub>2</sub> ) <sub>0.6</sub> [Eu(L) <sub>0.6</sub> (HL) <sub>0.4</sub> ]·0.4H <sub>2</sub> O	/	1.25	150	8
$\beta$ -PCMOF2(Tz) <sub>0.45</sub>	/	0.5	150	9

**Table S5.** List of proton conducting materials reported under high humidity at ambient temperature.

Compound	Proton conductivity (S cm <sup>-1</sup> )	E <sub>a</sub> (eV)	Conditions	Ref
H <sub>2</sub> SO <sub>4</sub> @MIL-101-SO <sub>3</sub> H (3 M)	1.82	0.39	70 °C, 90% RH	10
BUT-8(Cr)A	1.27 × 10 <sup>-1</sup>	0.11	80 °C, 100 % RH	11
PCMOF2½(Triazole)	1.17 × 10 <sup>-1</sup>	0.22	85 °C, 90 % RH	12
UiO-66-(SO <sub>3</sub> H) <sub>2</sub>	8.4 × 10 <sup>-2</sup>	0.32	80 °C, 90 % RH	13
Nafion	7.8 × 10 <sup>-2</sup>	0.22	25 °C, 100 % RH	14
TfOH@MIL-101	8.0 × 10 <sup>-2</sup>	0.23	15 °C, 60 % RH	15
Fe-CAT-5	5.0 × 10 <sup>-2</sup>	0.24	25 °C, 98 % RH	16
{[(Me <sub>2</sub> NH <sub>2</sub> ) <sub>3</sub> (SO <sub>4</sub> ) <sub>2</sub> [Zn(ox) <sub>3</sub> ]} <sub>n</sub>	4.2 × 10 <sup>-2</sup>	0.13	25 °C, 98 % RH	17
PCMOF10	3.6 × 10 <sup>-2</sup>	0.4	70 °C, 95 % RH	18
VNU-15	2.9 × 10 <sup>-2</sup>	0.22	95 °C, 60 % RH	19
ZrP	1.21 × 10 <sup>-2</sup>	0.30	90 °C, 95 % RH	This work
MIL-101-SO <sub>3</sub> H	1.16 × 10 <sup>-2</sup>	0.23	80 °C, 100 % RH	11
CPM-103a	1.0 × 10 <sup>-2</sup>	0.66	22.5 °C, 75 % RH	20
(NH <sub>4</sub> ) <sub>2</sub> (adp)[Zn <sub>2</sub> (ox) <sub>3</sub> ] 3H <sub>2</sub> O	8.0 × 10 <sup>-3</sup>		25 °C, 100 % RH	21
(Me <sub>2</sub> NH <sub>2</sub> )[Eu(L)]	3.76 × 10 <sup>-3</sup>	0.38	100 °C, 98% RH	8
UiO-66(Zr)-(CO <sub>2</sub> H) <sub>2</sub>	2.3 × 10 <sup>-3</sup>	0.17	90 °C, 95 % RH	22

## Supplementary References

1. Inukai, M.; Horike, S.; Itakura, T.; Shinozaki, R.; Ogiwara, N.; Umeyama, D.; Nagarkar, S.; Nishiyama, Y.; Malon, M.; Hayashi, A.; Ohhara, T.; Kiyanagi, R.; Kitagawa, S. *J. Am. Chem. Soc.* **2016**, *138*, 8505-8511.
2. Luo, H. B.; Ren, L. T.; Ning, W. H.; Liu, S. X.; Liu, J. L.; Ren, X. M. *Adv. Mater.* **2016**, *28*, 1663-1667.
3. Ponomareva, V. G.; Kovalenko, K. A.; Chupakhin, A. P.; Dybtsev, D. N.; Shutova, E. S.; Fedin, V. P. *J. Am. Chem. Soc.* **2012**, *134*, 15640-15643.
4. Ogiwara, N.; Inukai, M.; Itakura, T.; Horike, S.; Kitagawa, S. *Chem. Mater.* **2016**, *28*, 3968-3975.
5. Tang, Q.; Liu, Y.; Liu, S.; He, D.; Miao, J.; Wang, X.; Yang, G.; Shi, Z.; Zheng, Z. *J. Am. Chem. Soc.* **2014**, *136*, 12444-12449.
6. Umeyama, D.; Horike, S.; Inukai, M.; Hijikata, Y.; Kitagawa, S. *Angew. Chem. Int. Ed.* **2011**, *50*, 11706-11709.
7. Umeyama, D.; Horike, S.; Inukai, M.; Kitagawa, S. *J. Am. Chem. Soc.* **2013**, *135*, 11345-11350.
8. Wei, Y.-S.; Hu, X.-P.; Han, Z.; Dong, X.-Y.; Zang, S.-Q.; Mak, T. C. W. *J. Am. Chem. Soc.* **2017**, *139*, 3505-3512.
9. Hurd, J. A.; Vaidhyanathan, R.; Thangadurai, V.; Ratcliffe, C. I.; Moudrakovski, I. L.; Shimizu, G. K. H. *Nat. Chem.* **2009**, *1*, 705-710.
10. Li, X.-M.; Dong, L.-Z.; Li, S.-L.; Xu, G.; Liu, J.; Zhang, F.-M.; Lu, L.-S.; Lan, Y.-Q. *ACS Energy Letters* **2017**, *2*, 2313-2318.
11. Yang, F.; Xu, G.; Dou, Y.; Wang, B.; Zhang, H.; Wu, H.; Zhou, W.; Li, J.-R.; Chen, B. *Nat. Energy* **2017**, *2*, 877-883.
12. Kim, S.; Joarder, B.; Hurd, J. A.; Zhang, J.; Dawson, K. W.; Gelfand, B. S.; Wong, N. E.; Shimizu, G. K. H. *J. Am. Chem. Soc.* **2018**, *140*, 1077-1082.
13. Phang, W. J.; Jo, H.; Lee, W. R.; Song, J. H.; Yoo, K.; Kim, B.; Hong, C. S. *Angew. Chem. Int. Ed.* **2015**, *54*, 5142-5146.
14. Sone, Y.; Ekdunge, P.; Simonsson, D. *J. Electrochem. Soc.* **1996**, *143*, 1254-1259.
15. Dybtsev, D. N.; Ponomareva, V. G.; Aliev, S. B.; Chupakhin, A. P.; Gallyamov, M. R.; Moroz, N. K.; Kolesov, B. A.; Kovalenko, K. A.; Shutova, E. S.; Fedin, V. P. *ACS Appl. Mater. Inter.* **2014**, *6*, 5161-5167.
16. Nagarkar, S. S.; Unni, S. M.; Sharma, A.; Kurungot, S.; Ghosh, S. K. *Angew. Chem. Int. Ed.* **2014**, *53*, 2638-2642.
17. Ramaswamy, P.; Wong, N. E.; Gelfand, B. S.; Shimizu, G. K. H. *J. Am. Chem. Soc.* **2015**, *137*, 7640-7643.

19. Tu, T. N.; Phan, N. Q.; Vu, T. T.; Nguyen, H. L.; Cordova, K. E.; Furukawa, H. *J. Mater. Chem. A* **2016**, *4*, 3638-3641.
20. Zhai, Q. G.; Mao, C.; Zhao, X.; Lin, Q.; Bu, F.; Chen, X.; Bu, X.; Feng, P. *Angew. Chem. Int. Ed.* **2015**, *54*, 7886-7890.
21. Sadakiyo, M.; Yamada, T.; Honda, K.; Matsui, H.; Kitagawa, H. *J. Am. Chem. Soc.* **2014**, *136*, 7701-7707.
22. Borges, D. D.; Devautour-Vinot, S.; Jobic, H.; Ollivier, J.; Nouar, F.; Semino, R.; Devic, T.; Serre, C.; Paesani, F.; Maurin, G. *Angew. Chem. Int. Ed.* **2016**, *128*, 3987-3992.